Space–time prism and accessibility incorporating monetary budget and Mobility-as-a-Service

Please check the document version of this publication:

• A submitted manuscript is the version of the article upon submission and before peer-review. There can be important differences between the submitted version and the official published version of record. People interested in the research are advised to contact the author for the final version of the publication, or visit the DOI to the publisher's website.
• The final author version and the galley proof are versions of the publication after peer review.
• The final published version features the final layout of the paper including the volume, issue and page numbers.

[Link to publication](#)

Space–time prism and accessibility incorporating monetary budget and mobility-as-a-service

Jing Qin & Feixiong Liao

Published online: 10 Jan 2024.

Submit your article to this journal ⧉

Article views: 318

View related articles ⧉

View Crossmark data ⧉

Taylor & Francis
Taylor & Francis Group

RESEARCH ARTICLE

🔓 OPEN ACCESS

Check for updates

Space–time prism and accessibility incorporating monetary budget and mobility-as-a-service

Jing Qin and Feixiong Liao

Urban Planning and Transportation Group, Eindhoven University of Technology, Eindhoven, Netherlands

ABSTRACT

Recent years in time geography have witnessed a flourishment of space–time prism (STP) modeling extensions for enhancing realism. However, there is little research on the incorporation of monetary budget in STP models to capture personal potential mobility space more realistically. This study considers both time and monetary budget constraints in STP modeling in a multimodal supernetwork integrating mobility-as-a-service and trip chains. We develop an efficient two-stage bi-criterion bidirectional search method to identify Pareto path sets to construct the resulting STP for conducting a flexible activity between two anchor nodes. To demonstrate the effectiveness of the proposed model and solution method, a case study with varying scenarios is conducted to evaluate the impacts of monetary budget on space–time accessibility and equality. The findings show that the ignorance of monetary budget overestimates accessibility and that MaaS, if not well designed, may not improve equality in accessibility as intended.

1. Introduction

Space–time prism (STP) has been a core concept in time geography since it was first proposed by Hägerstrand (1970) as an envelope encompassing all possible space–time paths between two anchor nodes to perform a flexible activity. The spatially scattered locations and travel time budget forge the essential space–time constraints and accessibility. The projected STP on the planar space, called potential path area (PPA), includes all accessible locations. Given this appealing feature, STP has many applications for measuring space–time accessibility and delineating choice sets. Since the early work of Miller (1991) that extended the STP modeling over transport networks to consider varying link travel speeds, the field has flourished with STP modeling extensions to capture space–time constraints realistically.

CONTACT Feixiong Liao ✉ j.qin@tue.nl, f.liao@tue.nl

While the classical STPs have deterministic link travel times and anchor nodes, recent extensions of STP modeling attempt to relax such conditions. For instance, Chen et al. (2013) proposed a computational model to construct an STP with on-time arrival probabilities in road networks. Zhang et al. (2018) proposed an efficient routing algorithm considering both travel time uncertainty and service reliability to measure transit accessibility in large-scale multimodal transit networks. As travelers have different safety margins for routing strategies, Lee and Miller (2020) measured robust accessibility to deal with travel time uncertainty. Other than focusing on uncertain travel time, Kuijpers et al. (2010) suggested the concept of anchor regions that contain possible locations for anchor nodes with probabilities. By relaxing the assumption of isotropic space within the STP, a batch of studies applied the notion of visit probability to model space heterogeneities. Specifically, Winter and Yin (2010) applied the random walk theory to model visit probability within a planar STP, which was extended by Song et al. (2017) modeled visit probability in road networks using semi-Markov processes for measuring green space–time accessibility.

Another prominent line of development concerns the extended choice facets beyond a single transport mode, a single flexible activity, or a single person. For multimodal STP, most studies focused on multimodality interconnecting walking and one primary transport mode, for example, public transport (O'Sullivan et al. 2000, Widener et al. 2015) or private car (Yin et al. 2020). Based on a multimodal supernetwork representation, Qin and Liao (2021) proposed an effective method allowing for flexible trip chaining of walking, private vehicles, and public transport. For multi-activity STP, Kang and Chen (2016) suggested a method that first unites all location-specific space–time regions of an activity and subsequently intersects all these regions of multiple activities in an activity program. Using the multi-state supernetwork representation, Liao (2019, 2021) proposed efficient methods to construct exact STPs for conducting multiple activities. For multi-person STP, Neutens et al. (2007) determined the interaction spaces for a group of individuals traveling at different speeds and visualized their space–time intersections by a hybrid system. Fang et al. (2011) proposed a multi-objective solution method to schedule a joint activity for multiple individuals subject to respective space–time constraints. To assess joint space–time accessibility through public transit, Fu et al. (2022) proposed a method to identify feasible alighting locations considering joint activity choices and travel time uncertainty.

Besides the above extensions, there are other types of STP models, such as kinetic, realizable, and virtual STPs that enhance realism in travel speed, travel time, and choice facets respectively. Despite using different mechanisms, all STP models have common applications in geographic information systems to measure accessibility and/or inequality. For instance, Horner and Wood (2014) introduced a novel approach to measuring space–time accessibility at the individual level considering activity patterns and available time budgets. This method allows inter-person comparison and accessibility aggregation, making it possible to identify areas with high accessibility to services. Qin and Liao (2022) constructed STPs in a multimodal supernetwork to identify the inequality distribution of space–time accessibility to shopping and leisure opportunities in the Rotterdam–The Hague metropolitan area, the Netherlands. They found

that private vehicles enhance accessibility and mitigate the inequalities due to residential location disparities, even in the two cities with well-established public transport.

STP is powerful for describing an individual's potential mobility space and offers an instrumental measurement of space–time accessibility. Since the STP model inputs are individual-specific, the accessibility measurement is person-based and naturally respects individual heterogeneities, which offers a crucial tool for human-centric planning on top of the traditional place-based measurement. The existing STP models exclusively focus on space–time constraints and are capable of modeling spatial heterogeneities (for example, where an individual lives) and temporal heterogeneities (for example, how much time is available for an individual). However, due to the ignorance of other dimensions of resource constraints, the space–time accessibility measurement tends to overestimate accessibility and falls short of capturing heterogeneities. For example, without the consideration of monetary budget constraints, a rich individual and a poor individual would have the same accessibility to restaurants if they lived in the same neighborhood and had the same available time, which contradicts the reality that the rich usually can access more options. This sharp example echoes the recent equality analyses that emphasized the vital role of monetary costs in identifying disparities in accessibility of socially disadvantaged groups (El-Geneidy *et al*. 2016, Bittencourt and Giannotti 2021, Herszenhut *et al*. 2022). In geography and urban planning, much research has already revealed that travel time and monetary costs impact accessibility to opportunities (Handy and Niemeier 1997, Ford *et al*. 2015, Conway and Stewart 2019). In addition, it is well-documented in the consumer surplus measure of accessibility (Ben-Akiva and Lerman 1979) that individual potential mobility is influenced by multiple factors including the use of time and money. Therefore, it is argued that from the constraint-based point of view, potential mobility space is in principle limited by multiple resources, of which time and money are two pivotal resources. To the best of our knowledge, Mahmoudi *et al*. (2019) was the only study that explicitly incorporated multiple resource-based constraints into the construction of STPs. Specifically, they extended STP to a hyper-prism that encompasses time and other resource constraints in an expanded space–time network. However, their STP model concerns the intersection of multiple separate resource-based STPs. This method is applicable only if there is consistency in the expenses of multiple resources across links. For example, the emissions are calculated proportional to the time expenses on the corresponding links. The stipulated problem may, unfavorably, be simplified by merging multiple constraints into one single constraint. Additionally, although their model can account for different transport modes as a distinct resource constraint, it is unable to accommodate flexible trip chaining due to the lack of a unified multimodal representation, particularly with regard to the use of private vehicles that require pick-ups before returning to destinations.

This study aims to propose an STP model extension, referred to as STP_M, that simultaneously accounts for both space–time and monetary constraints. Likewise, the resulting projection of STP_M onto the planar space, known as PPA, includes all reachable locations satisfying the required constraints. In addition, an efficient search method is developed to construct STP_M in a multimodal transport network. Regarding multimodality, we incorporate mobility-as-a-service (MaaS) which has attracted

considerable attention for its potential to stimulate sustainable mobility and improve equality by reducing the ownership and use of private cars (Hietanen 2014). MaaS provides bundled mobility services of multimodality through subscriptions in a digital channel. For that reason, MaaS exhibits a complex cost structure, making it an ideal testbed for assessing the effects of monetary budget. To that effect, we first apply the multimodal supernetwork representation (Qin and Liao 2021) to integrate MaaS, referred to as SNK_M, for capturing the simultaneous mode and route choice. In SNK_M, we suggest a generic monetary cost structure based on the MaaS schemes at the link and path levels. Then, we develop an efficient two-stage bi-criterion bidirectional search (TBBS) algorithm for constructing STP_M in SNK_M. In the search process, the algorithm considers both time and monetary expenses and constraints to efficiently generate Pareto space–time paths in SNK_M in pseudo-polynomial running time. A case study is performed in the Eindhoven-Helmond corridor (the Netherlands) to demonstrate the effectiveness of the proposed method and the potential of applications for measuring accessibility and equality. The results show that ignoring monetary budget tends to overestimate space–time accessibility and that MaaS holds the promise of improving accessibility and equality only if the improvement in accessibility caused by the introduction of MaaS is directed to those who suffer from low accessibility.

The remainder of this paper is organized as follows. The next section provides STP_M formulations in SNK_M. In what follows, Section 3 presents the TBBS algorithm to construct STP_M, and Section 4 discusses the case study for applications of STP_M. Finally, Section 5 concludes the paper and provides avenues for future work.

2. Space–time prism incorporating monetary budget and MaaS

This section presents the formulations for constructing STP_M in SNK_M to participate in a single flexible activity between two anchor nodes (see primary notations and definitions in the Appendix Table A1). We start with the preliminary knowledge of the classic STP in a multimodal transport network and then integrate MaaS into a multimodal supernetwork to form SNK_M. Next, we formulate a generic cost structure for MaaS and adapt the STP_M formulation accordingly. Lastly, we suggest the measurements of space–time accessibility and equality with monetary budget.

2.1. STP and STP_M formulations

The classic STP describes an individual's potential mobility to engage in a flexible activity with a single transport mode under a time budget. In transport network G, the condition for node n falling within the PPA can be expressed as the sum of minimum travel times between node n and the two anchor nodes being no greater than the remaining travel time budget.

In the multimodal transport context, private vehicle networks (PVNs) and public transport networks (PTNs) are basic network units for constructing multimodal supernetworks (Liao et al. 2010, 2013). A PVN can be accessed only by the related private vehicle (PV), and a PTN can be accessed by walking and public transport (PT). PTNs are constructed based on the timetables of public transit, where all in-vehicle links

and transfer links have time tags. In the PVN, link time expenses can be derived by the lengths and average travel speeds of a transport mode along the links. In the PTN, the time expense of a transit link between two consecutive stops, despite possibly traversing multiple streets, is represented as one elementary link. Their time expenses are calculated by subtracting departure times from arrival times as specified in the timetable data. Each network unit is assigned with vehicle state p indicating if PV is being used or parked at a specific parking place, and activity state s indicating if the flexible activity has been conducted (0: unconducted; 1: conducted). PV includes all accessible private transport modes by the individual at h_0, e.g. PV = {car, bike}; PT includes the traditional public transport modes, such as bus, metro, and train. Once a PV is used, the PV should be returned to h_1 after the activity is conducted. Transfers between PV and PT modes are represented by transfer links switching vehicle states between PVNs and PTNs. The waiting time at a station can be determined based on the arrival time and the next departure PT vehicle at the station. Transaction links represent activity participation switching activity states. An individual's physical movements in the supernetwork need to traverse travel links inside PTNs and/or PVNs. Under all these setups, the multimodal supernetwork (Figure 1) can represent all space−time paths for an individual to participate in a flexible activity. Flexible trip chaining between multiple transport modes can be accommodated in the multimodal supernetwork.

The condition that node n with transport mode m at activity state s and vehicle state p, denoted by $n|_{sp}^m$, falls inside the STP is formulated as

$$\tau_c\left(h_0, n|_{sp}^m\right) + \tau_c\left(n|_{sp}^m, h_1\right) \leq b_c, \ c = T \tag{1}$$

where h_0 and h_1 denote the start and end anchor nodes, respectively; $n|_{sp}^m$ ($s = 0$ or $s = 1$) refers to node n with m at vehicle state p either before or after activity participation in the multimodal supernetwork, respectively; $\tau_T\left(h_0, n|_{sp}^m\right)$ and $\tau_T\left(n|_{sp}^m, h_1\right)$ denote the minimum time expenses between node $n|_{sp}^m$ and the two anchor nodes; b_T is the given time budget; the minimum activity duration d_T on a transaction link is
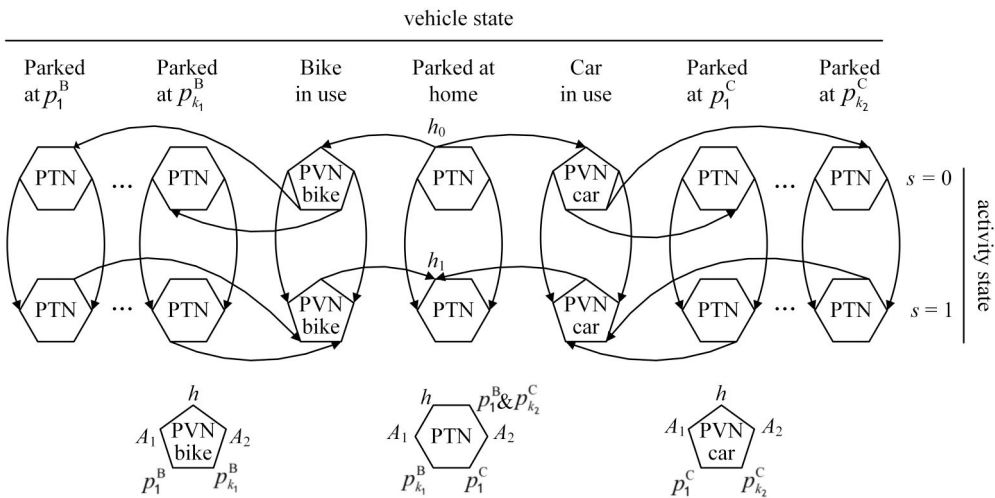

Figure 1. Multimodal supernetwork (Qin and Liao 2021).

implicitly included in one of the two subpaths between $n|_{sp}^{m}$ and the two anchor nodes. It's important to clarify that the notation 'n' indeed represents a node in the physical network, whereas $n|_{sp}^{m}$ represents a node in the supernetwork characterized by activity state 's', vehicle state 'p', and the used transport mode m. The extension from n to $n|_{sp}^{m}$ enables us to incorporate complicated trip chains for the STP modeling. Equation (1) can be solved by applying twice one-to-all shortest path searches from the two anchor nodes. It is noteworthy that the backward search from h_1 should be conducted in the reversed multimodal supernetwork.

In addition to the traditional PT, MaaS encompasses a variety of shared mobility services (SMSs), such as shared cars and micro-mobility (including bikes and scooters, etc.). Although some vehicle types (e.g. bike and car) seem duplicated in both PV and MaaS, PV is distinguished from MaaS by the requirement of being picked up (if used) after conducting the activity. To incorporate MaaS into the supernetwork, we create a multi-layer network of MaaS in Figure 2(a), in which each layer is accessible by a unique SMS and connected to other layers by transfer links between them. For MaaS modes, the average waiting time is allocated on the transfer link as well, whose values are determined by the deployment of MaaS, a high level of deployment leading to less average waiting time, and vice-versa. While PVs and SMSs use the same mode-specific road network, PTN is represented in a time-expanded network based on the PT timetable. Following the supernetwork terminologies, the individual switches MaaS modes by crossing different layers of MaaS (Figure 2(a)) and changes activity states by crossing two MaaS networks (Figure 2(b)). After embedding a MaaS network in Figure 2 as a PTN in Figure 1, the property that all space–time paths are encompassed in the multimodal supernetwork still holds, and so does condition Equation (1) for the STP.

Motivated by the fact that an individual's potential mobility space is also constrained by monetary budget, we extend the multimodal supernetwork to include monetary costs, denoted as SNK_M. Monetary expenses often have complex cost structures and cannot be obtained directly, especially for different MaaS pricing bundles. Below we define a monetary cost structure in SNK_M using link incidences at a path level. Consider path ρ from h_0 to arbitrary node n has J links, e_j ($j = 1, \ldots., J$), where
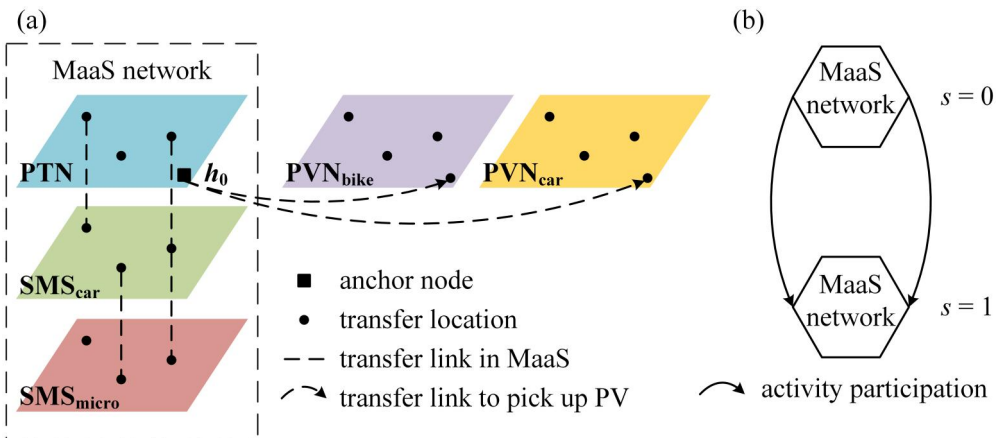

Figure 2. (a) MaaS with transfers; (b) change of activity states.

e_1 and e_J are the first and last links of ρ. The monetary cost $\varpi^m_{e_jM}$ traversing link e_j with transport mode m is formulated as

$$\varpi^m_{e_jM} = \alpha^m_{\rho e_j} \cdot F^m_M + \sum_c \beta^m_{e_jc} \cdot \delta^m_c \cdot \varpi^m_{e_jc}, \quad c \in \{T, L\} \tag{2a}$$

$$\alpha^m_{\rho e_j} = \begin{cases} 1, & \text{if } j = \arg\min_{j'} \{e_{j'} \in E^m_\rho\}, \ j' \leq j \\ 0, & \text{otherwise} \end{cases} \tag{2b}$$

$$\beta^m_{e_jc} = \begin{cases} 1, & \text{if } \sum_{j'=1}^{j} \gamma^m_{e_{j'}} \cdot \varpi^m_{e_{j'}c} > \theta^m_c , \gamma^m_{e_{j'}} = 1, \ c \in \{T, L\} \\ 0, & \text{otherwise} \end{cases} \tag{2c}$$

where $\alpha^m_{\rho e_j}$ is a path-level binary indicator, equal to 1 if e_j is the first transfer link in ρ to take transport mode m, and 0 otherwise; E^m_ρ denotes the set of transfer links to use transport mode m in ρ; F^m_M is the fixed (base) fee associated with using transport mode m; $\beta^m_{e_jc}$ is a path-level binary indicator showing if e_j is an in-vehicle link beyond the range of free use of transport mode m in time or length; $\gamma^m_{e_{j'}}$ is a binary indicator, equal to 1 if $e_{j'}$ is an in-vehicle link using transport mode m and 0 otherwise, where $e_{j'}$ can be a link in any link type along the path ρ between the first link (e_1) to the current link e_j; θ^m_c is a predefined amount of free use of transport mode m in cost type c, $c \in \{T, L\}$, in terms of time and distance; δ^m_c is a coefficient converting two link cost types into monetary cost. For example, for a scenario involving a one-time fixed purchase with free transfers, the one-time purchase fee is presented as a fixed cost (F^m_M), $\alpha^m_{\rho e_j}$ is restricted to 1 once for all transport modes, θ^m_c is assigned with large values. In this article, unless stated otherwise, 'M' refers to monetary cost and 'm' to transport mode. Based on Equation (2a–c), the total monetary cost of ρ is formulated as

$$\ell_{\rho c}(h_0, n) = \sum_m \sum_{e_j} \varpi^m_{e_jc}, \quad c = M \tag{3}$$

Based on the time and monetary costs defined in SNK_M, a node $n|^m_{sp}$ inside the STP_M if there exists a path ρ (between h_0 and h_1) consisting of two sub-paths ρ_1 (between h_0 and $n|^m_{sp}$) and ρ_2 (between $n|^m_{sp}$ and h_1) in SNK_M satisfying the following condition

$$\ell_{\rho_1 c}\left(h_0, n|^m_{sp}\right) + \ell_{\rho_2 c}\left(n|^m_{sp}, h_1\right) \leq b_c, \quad c \in \{T, M\} \tag{4}$$

where $\ell_{\rho_1 c}\left(h_0, n|^m_{sp}\right)$ and $\ell_{\rho_2 c}\left(n|^m_{sp}, h_1\right)$, $c \in \{T, M\}$, denote the travel costs (in terms of time and money) associated with ρ_1 and ρ_2 respectively, either of which includes d_c as the minimum cost of the flexible activity in a transaction link; b_c is the given travel budget. It should be noted that the travel costs in Equation (4) are not necessarily the minimum costs because of the dual constraints. Any node inside the STP_M in a path ρ between h_0 and h_1 should have time and monetary expenses no greater than the corresponding budgets. For any node $n|^m_{sp}$ satisfying Equation (4), the STP_M can be represented as a set of time and monetary intervals delineating the accessible time and monetary windows at all nodes as

$$STP_M = \bigcup_\rho \left\{ \left[w_{c0} + \ell_{\rho_1 c}\left(h_0, n|^m_{sp}\right), w_{c1} - \ell_{\rho_2 c}\left(n|^m_{sp}, h_1\right) \right], \ n|^m_{sp} \in \rho, c \in \{T, M\} \right\} \tag{5}$$

where w_{c0} is the initial cost point in terms of time and money at h_0, $w_{c1} = w_{c0} + b_c$, $c \in \{T, M\}$. At h_0, w_{T0} is the earliest departure time and w_{M0} is set to zero. Equation (5) details the time and monetary windows for any accessible node through a space−time path satisfying Equation (4).

2.2. Accessibility and equality measures

STP has been extensively employed for evaluating space−time accessibility. We apply two common accessibility measures in Equations (6) and (7), namely, the number of accessible locations (NAL) and aggregate flexible costs (AFC_c) in terms of time and monetary expenses (Neutens et al. 2010, Qin and Liao 2022).

$$NAL = \sum_a \chi(a), \quad \chi(a) = \begin{cases} 1, & if \ a \ \in STP_M, \ a \ \in A \\ 0, & otherwise \end{cases} \tag{6}$$

$$AFC_c = \sum_a \max_\rho \left(b_c - \ell_{\rho_1 c}\left(h_0, a|_{sp}^m\right) - \ell_{\rho_2 c}\left(a|_{sp}^m, \ h_1\right) \right), a \in STP_M, \ c \in \{T, \ M\} \tag{7}$$

where $\chi(a)$ is a binary indicator showing if activity location a is accessible (0: inaccessible; 1: accessible); AFC_c refers to the sum of the maximum remaining time and monetary budgets for each accessible activity location after reaching h_1. We choose the Gini coefficient (Gini 1909) as an inequality (opposite of equality) indicator to evaluate the accessibility distribution among a population. The Lorenz curve is an accompanying graphical analysis tool showing the cumulative distribution of accessibility among the population. Assuming there are I discrete samples on the Lorenz curve (x_i, y_i), $i = 1, \ldots, I$, the Gini coefficient can be approximated as

$$GINI = 1 - \sum_{i=1}^{I-1} (x_{i+1} - x_i)(y_{i+1} + y_i) \tag{8}$$

where x_i is the cumulated share of the population and y_i is cumulated accessibility along the Lorenz curve with $x_1 = 0$, $y_1 = 0$, and $x_I = 1$, $y_I = 1$. The Gini coefficient, ranging from 0 to 1, shows the gap between the actual distribution of cumulated accessibility to the perfect distribution line, with 0 meaning the perfect equality and 1 the most inequality. Constrained by both time and monetary budgets, the above formulations enable the measurements of space−time accessibility with the addition of monetary budget at the individual level and the associated equality at the population level.

3. Two-stage bi-criterion bidirectional search in SNK_M

For constructing STP_M, an intuitive method, as adopted by Mahmoudi et al. (2019), is to first construct STP and space-money prism (SMP) separately and then intersect them. Similar to STP, SMP is an envelope encompassing all potential space-money paths between two anchor nodes to participate in a flexible activity, and the projected SMP on the planar space (or PPA) encompasses all accessible locations subject to the monetary budget constraints. However, as we demonstrate in an example network below, this intuitive solution fails to obtain the correct STP_M. Accordingly, we develop

a two-stage bi-criterion bidirectional search (TBBS) method to construct the correct STP_M.

3.1. An intuitive search method

The Dijkstra algorithm and its variants of the label-setting method are commonly applied to construct the STP for a single criterion. When dealing with multiple resource constraints, a plausible approach involves intersecting the respective prisms for single resource budgets. The procedure begins with constructing an STP satisfying a given time budget, within which space−time paths satisfying monetary budget are identified as STP_M.

Figure 3(a) shows the link numbers and costs (*time expense, monetary expense*) in a toy network. Considering a time budget of 20 minutes and a monetary budget of 5 euros. Figure 3(b) shows the accessible budget windows as $[o_{Tn}, u_{Tn}]/[o_{Mn}, u_{Mn}]$, $n \in \{n_1, n_2, n_3\}$, where o_{cn} and u_{cn}, $c \in \{T, M\}$, are the earliest/lowest arrival and the latest/highest departure respectively at node n in terms of time and money through different space−time paths between h_0 and h_1. As shown, some paths ($e_1 - e_2$ and $e_5 - e_6$) only meet the time budget, some paths ($e_4 - e_6$ and $e_7 - e_8$) only meet the monetary budget, and only one path ($e_3 - e_6$) meets both the time and monetary budget constraints at n_2. It is evident that nodes n_1 and n_2 fall within the STP, while nodes n_2 and n_3 fall within the SMP. Consequently, their intersection comprises node n_2 with accessible time and monetary budget windows as [5, 12] and [2, 4] respectively. However, these budget windows are generated by two paths ($e_5 - e_6$ and $e_4 - e_6$) separately. As dictated by Equation (4), a node needs to satisfy the two cost constraints simultaneously via the same space−time path. In the actual STP_M, node n_2 has an accessible budget window [8, 12] for time and [3, 4] for money by path $e_3 - e_6$, which differs from the intersected budget windows.

By varying the link costs in the example network, it is even possible to encounter a situation where the intersection of STP and SMP has a non-empty PPA, while the STP_M is empty. The intersection method is valid only when the network has consistent time and monetary expenses in all paths, for example, $\ell_{\rho M}$ equal to a linear multiple of $\ell_{\rho T}$, which may not hold in realistic networks. As illustrated above, path enumeration
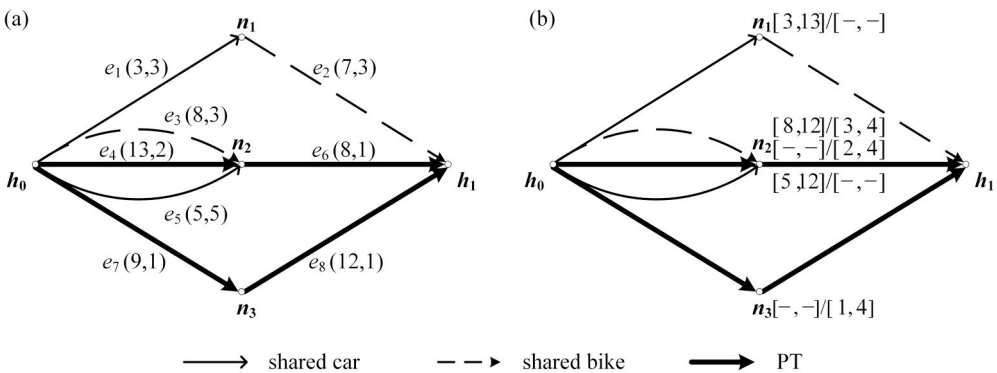

Figure 3. (a) Example network with link costs; (b) budget window for n_1, n_2, and n_3.

allows us to check multiple resource constraints simultaneously, but it is not feasible in large-scale transport networks. The existing bi-criterion shortest path search methods through path extensions offer a viable solution to construct STP_M.

3.2. Bi-criterion search method to construct STP_M

The proposed TBBS builds upon the efficient methods introduced by Hernández Ulloa *et al.* (2020) for the bi-criterion shortest path search and Liao (2021) for the two-stage search. While Hernández Ulloa *et al.* (2020) focused on bi-criterion shortest paths and Liao (2021) aimed at finding the single criterion STP, this study aims to pinpoint the bi-criterion STP_M in SNK_M.

In Hernández Ulloa *et al.* (2020), the so-called lazy dominance is proposed to assess dominance relationships between various paths from the start anchor node and any search frontier node. In bi-criterion search, a label refers to a two-tuple vector recording the two-criterion costs following a path. The method employs pre-allocated space to store non-dominated labels of paths grouped by the discretized time expenses as the first criterion. In each group, labels are ranked in ascending order based on the second-criterion cost. For each node, there is a temporary variable recording the latest identified non-dominant label. In this way, the number of dominance checks for each node is significantly reduced as it requires only a single comparison between the newly generated label and the latest identified non-dominated label, rather than comparing with all existing non-dominated labels. In Liao (2021), the forward search starts from h_0 with an admissible lower bound estimation of cost between a search frontier node and h_1. The forward search space is determined by the quality of the lower bound, and the backward search corresponds to the actual PPA.

We apply three speedup techniques to accelerate the search process. First, the search space in SNK_M is limited in the intersection area of STP and SMP, which are created as a preprocessing step. The intersection area is considered an upper bound of the search space. Second, goal-directed search is implemented in the first stage (forward search from h_0) to reduce the search space, for which the actual minimum costs obtained from creating STP and SMP are used as the lower bound costs. Third, we use a slack value of time to eliminate inferior non-dominated labels (corresponding to Pareto sub-paths) at intermediate nodes with little compromise of the solution quality (Goldin and Salzman 2021).

In the forward search, a lower bound cost from the search frontier node to the end anchor node in SNK_M is used to guide the search toward the destination. Equation (9) defines the forward search space.

$$\vec{\ell}_{\rho_1 c}\left(h_0, n|_{sp}^m\right) + \vec{\xi}_c\left(n|_{sp}^m, h_1\right) \leq b_c, \ c \in \{\text{T, M}\} \tag{9}$$

where $\vec{\xi}_c\left(n|_{sp}^m, h_1\right)$ is a lower-bound estimation of $\vec{\ell}_{\rho_2 c}\left(n|_{sp}^m, h_1\right)$ in Equation (4), and the arrows above the notations indicate the forward search direction. The estimated cost from h_0 via $n|_{sp}^m$ to h_1, $\vec{f}_{\rho c}$, is equal to $\vec{\ell}_{\rho_1 c}\left(h_0, n|_{sp}^m\right) + \vec{\xi}_c\left(n|_{sp}^m, h_1\right)$. The backward search is delineated by Equation (4), a tighter condition than Equation (9). Thus, the backward search space is in principle smaller than the forward search space. Figure 4 schematically shows the area of STP and SMP as well as their intersection

(Figure 4(a)) and the search space of STP_M (Figure 4(b)) with h_0 and h_1 as the anchor nodes. In Figure 4(b), n_1 and n_2 are located at the borders of forward and backward search spaces, respectively. Given a tight monetary budget, the final STP_M is usually located inside the intersection of STP and SMP.

TBBS finds a set of Pareto paths from h_0 to a search frontier node n in SNK_M. Each Pareto path is presented as the k-th non-dominated label of node n, $q_k(n)$, which stores $\ell_{p_1c}(h_0, n)$, estimated cost $f_{pc}(n)$, parent node $\mathscr{p}_k(n)$ of n, and the number of transfers $z_k(n)$ to reach n. The exploration of the search frontier is facilitated by two containers, denoted as Γ_f and Γ_b, which store labels for the forward and backward search, respectively. The counts of labels of n in Γ_f and Γ_b is represented as $|\Gamma_f(n)|$ and $|\Gamma_b(n)|$, respectively. A bucket data structure is applied to store labels in Γ_f and Γ_b. The discretized time expenses of all explored p_1 as well as the corresponding f_{pT} are sorted in ascending order and those labels with the same f_{pT} are stored in the same bucket, in which the labels are sorted in ascending order of f_{pM}.

For initialization (lines 1–3), the first label is generated for h_0 and inserted into the first bucket of Γ_f. The storage strategy introduced above enables the extraction of labels in a lexicographical manner by retrieving and deleting the first label from the first non-empty bucket (line 5) in Γ_f. For each new label to be added, a lazy-check strategy is employed to determine the dominance relationship between this label and only one label of the same node that has been identified with the minimum $\ell_{p_1M}(h_0, n)$ recorded as $\vartheta_M(n)$ of $\vartheta_c(n)$ in line 7. Since f_{pT} is explored in ascending order, the new label is non-dominated only when $\ell_{p_1M}(h_0, n) < \vartheta_M(n)$. This approach significantly reduces the number of comparisons (taking constant time), compared to the classical bi-criterion search where each new label needs to be compared with all the extant non-dominated labels of the same node (taking linear time with the size of the non-dominated set).

To further reduce the non-dominated labels of n, an individual-specific Q is used in the dominance check (line 6). The updated dominance check is: $q_k(n)$ is not dominated if and only if conditions $\mathbf{C}_1(n)$: $\overrightarrow{\ell}_{p_1M}(h_0, n) + Q \cdot \left(\overrightarrow{\ell}_{p_1T}(h_0, n) - \overrightarrow{\vartheta}_T(n) \right) < \overrightarrow{\vartheta}_M(n)$ and $\mathbf{C}_2(n)$: $\overrightarrow{f}_{pM}(n) < \overrightarrow{\vartheta}_M(h_1)$ are satisfied. The inclusion of Q results in an approximation of the Pareto set with reduced non-dominant path labels. If $q_k(n)$ is
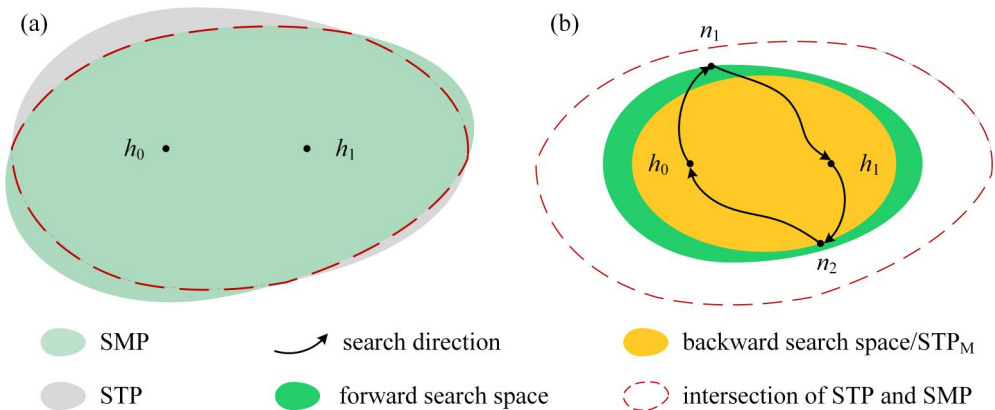

Figure 4. STP, SMP, STP_M, and search space of TBBS (drawn to scale).

Forward bi-criterion search
1   **Initialization:** $\overrightarrow{\vartheta}_M(n) = +\infty, |\Gamma_f(n)| = 0, \ \forall n \in V$; $\Gamma_f = \psi_f = \emptyset$;
2    $n = h_0, \ \overrightarrow{\ell}_{p_1c}(h_0, n) = (0,0), \ \not{p}_1(n) = h_0, \ \overrightarrow{f}_{pc}(n) = \overrightarrow{\ell}_{p_1c}(h_0, n) + \overrightarrow{\xi}_c(n, h_1), \ \overrightarrow{z}_1(n) = 0$;
3    $\overrightarrow{q}_1(n) = \left\langle \overrightarrow{\ell}_{p_1c}(h_0, n), \ \overrightarrow{f}_{pc}(n), \ \not{p}_1(n), \ \overrightarrow{z}_1(n) \right\rangle$; insert $\overrightarrow{q}_1(n)$ to $\Gamma_f, |\Gamma_f(n)| = 1$;
4   **while** $\Gamma_f \neq \emptyset$ **do**
5   extract $\overrightarrow{q}_k(n)$ with the lexicographically smallest f-value in Γ_f;
6   **if** $\overrightarrow{f}_{pc}(n) \leq b_c$ && $\mathbf{C}_1(n)$ && $\mathbf{C}_2(n)$
7   insert $\overrightarrow{q}_k(n)$ to ψ_f; $\overrightarrow{\vartheta}_c(n) = \overrightarrow{\ell}_{p_1c}(h_0, n)$;
8   **for** each $n^+ \in N^+(n)$
9        $j = |\Gamma_f(n^+)| + 1$;
10   **for** each $e(n, \ n^+)$
11         $\overrightarrow{\ell}_{p_1c}(h_0, n^+) = \overrightarrow{\ell}_{p_1c}(h_0, n) + \varpi_{ec}^m(n, n^+), \ \overrightarrow{f}_{pc}(n^+) = \overrightarrow{\ell}_{p_1c}(h_0, n^+) + \overrightarrow{\xi}_c(n^+, h_1)$;
12   **if** $e(n, \ n^+)$ is a transfer link, $\overrightarrow{z}_j(n^+) = \overrightarrow{z}_k(n) + 1$;
13   **if** $\overrightarrow{f}_{pc}(n^+) \leq b_c$ && $\mathbf{C}_1(n^+)$ && $\mathbf{C}_2(n^+)$ && $\overrightarrow{z}_j(n^+) \leq R$
14          $\not{p}_j(n^+) = n$, insert $\overrightarrow{q}_j(n^+)$ to Γ_f, sort the corresponding bucket in Γ_f, update $r(\Gamma_f)$;
15   **return** ψ_f
$\mathbf{C}_1(n):$ $\overrightarrow{\ell}_{p_1M}(h_0, n) + Q \cdot \left(\overrightarrow{\ell}_{p_1T}(h_0, n) - \overrightarrow{\vartheta}_T(n) \right) < \overrightarrow{\vartheta}_M(n)$ and $\mathbf{C}_2(n):$ $\overrightarrow{f}_{pM}(n) < \overrightarrow{\vartheta}_M(h_1)$.

non-dominated, it is stored in a container ψ_f, which is the container stores all non-dominant labels, and $\vartheta_c(n)$ is updated. Subsequently, the exploration of a successor node $n^+ \in N^+(n)$ of n starts (lines $8-14$), where $N^+(n)$ is a set of successor nodes of n. Each link to a successor node generates one label with a link cost ϖ_{ec}^m, which is inserted in Γ_f if it satisfies specific conditions (lines 13). The forward search is terminated when no node is active satisfying the budget constraints in lines 6 and 13 for extending the search frontier.

In the backward search, several modifications are made to the pseudo-codes of the forward search. First, the notations have a backward search direction replaced by $\leftarrow$, and the containers are changed to Γ_b and ψ_b. Second, lines 2–3 should be modified to include the insertion of $\overleftarrow{q}_k(h_1)$ with each label associated with h_1 in Γ_f, and $\overleftarrow{\ell}_{p_1c}(h_1, h_1) = (0,0)$, $\overleftarrow{f}_{pc}(h_1, h_0) = \overleftarrow{\ell}_{p_2c}(h_1, h_1) + \overrightarrow{\ell}_{p_1c}(h_0, h_1)$, $\not{p}_k(h_1) = h_1$. Third, $\overleftarrow{f}_{pc}(n^+)$ is updated to $\ell_{p_2c}(h_1, n^+) + \overrightarrow{\ell}_{p_1c}(h_0, n^+)$ in line 11. STP$_M$ is constructed for all nodes in ψ_b satisfying Equation (5). It is usually not straightforward to evaluate the running time complexity of the goal-directed search. However, since time is discretized and there is a time budget for conducting the activity, there is an upper bound in the number of labels. Suppose one unit of time (e.g. one minute) is discretized to N_T intervals equally, then the time budget b_T can be discretized into $b_T \cdot N_T$ intervals. Based on the rule of dominance, each time interval can have only one label at most; thus, the maximum number of labels per node is $N_L = b_T \cdot N_T$. The network units of the supernetwork, i.e. PTN and PVN, are sparse because of the low node degrees. The number of road segments or transit connections represented as links is only a few times larger than the number of road intersections or PT stops represented as nodes. For example, one road junction is typically linked with four road segments, i.e. a degree of four. Consequently, it follows that SNK_M, interconnecting PVNs and PTNs with transition links across different network units, is also sparse. For any extracted label of a node in sparse SNK_M, only a few neighboring nodes are explored.

Meanwhile, sorting is needed to add a new label to a sorted bucket, which has $O(\log N_s)$ running time. Taken together, the worst-case running time complexity is pseudo-polynomial with $O(N_s \cdot N_L \cdot \log N_s)$, where N_s is the number of nodes in SNK_M.

4. Case study

A case study is conducted to illustrate the applications of STP_M considering time and monetary budgets. To demonstrate STP_M at an individual level, we first illustrate the differences between STP, SMP, the intersection of STP and SMP, and STP_M. To demonstrate the applications at a population level, we measure space–time accessibility and equality. Below we first show the setup and then the analysis results of the case study.

4.1. Setup

We consider the participation in a common flexible activity, grocery shopping, during non-peak hours on a typical workday in Eindhoven-Helmond corridor, the Netherlands (Figure 5). There are 34 and 9 four-digit postcode areas in Eindhoven and Helmond, respectively, with 140 grocery stores in total corresponding to a variety of supermarkets. A sample of the population was extracted from the national mobility survey in 2019 from Centraal Bureau voor de Statistiek (CBS) and Rijkswaterstaat (RWS-WVL), including individual travel diaries and socio-demographic information. The sample was weighted to represent the entire population, including 2,327 residents aged 18–75 from ten income groups. For privacy protection, a random location within the same residential postcode area was assigned as the home location for each person. The
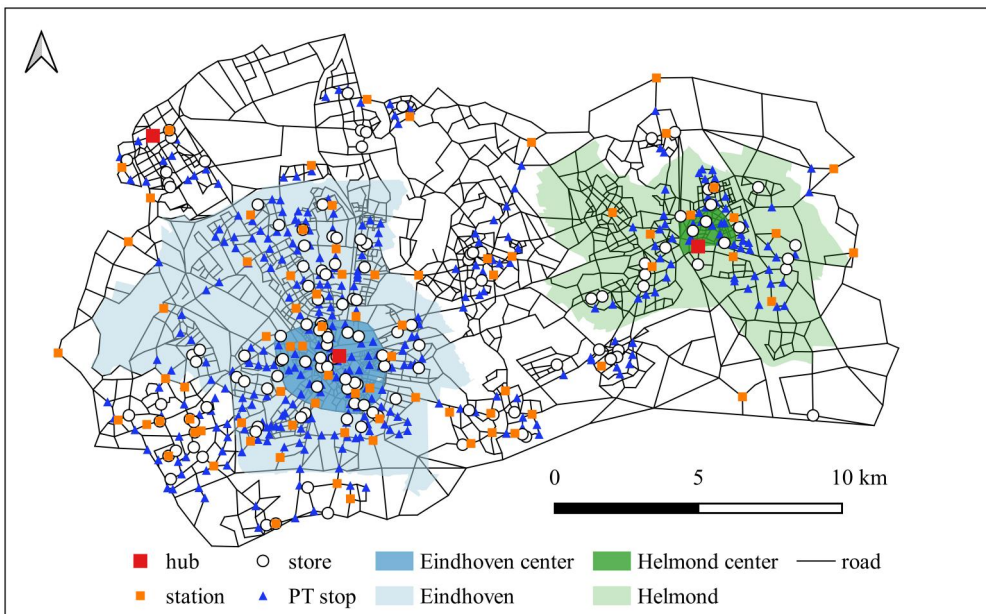

Figure 5. Study area.

travel time budget (60 min) and activity duration (30 min) were derived according to the average travel time budget and activity duration.

It is supposed that each person has access to MaaS and a private bike, while car ownership was extracted from the travel diary where 48% of the sample own cars. We evaluate the accessibility baselines using bike + PT and car (depending on car owner-ship). Typically, an individual's accessibility is equal to the maximum values based on Equations (6)–(8) considering all available mode alternatives. To illustrate the effects of monetary budgets and the introduction of MaaS, we also specify the accessibility associated with certain modes. The travel range of bike in trip chain bike + PT is restricted to 10 km, owing to physiological constraints. PTN is constructed based on the timetable from the general transit feed specification (GTFS). There are 485 PT stops with 43,030 basic PT connections, each of which includes the departure stop, end stop, start time, end time, line number, and trip number. All transfer locations for MaaS are restricted at PT stops. This setup is in line with the recently popular concept of smart hubs, which are typically placed near public transit stops. It's worth noting that the proposed space-–time prism model can address MaaS without the necessity of fixed stations in the free-floating scheme by adding transfer links at all possible locations within the MaaS network, which is not considered in the present case study. Based on the service frequency, three large PT stops (hub) and 59 medium-sized PT stops (station) are selected as parking and transfer stops. The road network for PVN was created from *OpenStreetMap* (https://www.openstreetmap.org) and categorized into five distinct road types: residential, local, local priority, regional, and motorway, while motorways are only accessible by motorized vehicles. Average travel speeds are assigned to the five road types respectively: private and shared cars ($<15, 30, 40, 50, 70>$ km/h), shared scooters ($<10, 15, 24, 36, 0>$ km/h), private and shared bikes ($<10, 12, 15, 18, 0>$ km/h), and walking ($<5, 5, 5, 5, 0>$ km/h). The road network has 4,242 links and 2,736 nodes.

Three MaaS bundles (Table 1) are evaluated. The first option operates as a pay-as-you-go service without a membership fee, while the other two options have mem-bership fees but reduced bundled prices compared to the first option. The parking fee is only applied to private cars and is determined based on the parking locations. The study area is classified into three types: center (dark blue and green areas in Figure 5), urban (light blue and green areas), and others (the remaining areas). The parking fees in these areas are €2.0, €1.0, and €0.0, respectively. For private bikes, we set the use and parking fees to €0.0.

Incorporating the above settings, a supernetwork is constructed based on a few well-defined strategies to select parking locations to capture consistent multimodal trip chaining between private vehicles and public transport (Qin and Liao 2021). Those strategies aim to remove transfer locations that do not contribute much to enlarging the action space for conducting the activities. Based on experimental results, Qin and

Table 1. MaaS bundle.

Bundle level	Membership fee (€/day)	F_M^m (€)			δ_T^m (€/h)			δ_L^m (€/km)
		SMS_{car}	SMS_{micro}	PT	SMS_{car}	SMS_{micro}	PT	SMS_{car}
Low	0.0	4.0	4.0	2.0	8.0	8.0	6.0	0.6
Medium	1.0	2.8	2.8	1.4	5.6	5.6	4.2	0.4
High	3.0	1.6	1.6	0.8	3.2	3.2	2.4	0.2

Liao (2021) demonstrated that the selection of locations scales down the size of the multimodal supernetwork and yields a noteworthy acceleration of computation speed by 1–2 orders of magnitude (around 50 times in terms of speedup) with little under-estimation in accessibility measurement.

4.2. Results

4.2.1. Demonstration at an individual level

We consider an individual who has a monetary budget of 12 euros, subscribes to the high MaaS bundle, and owns a medium-sized car. We focus on the comparison of accessibility associated with using the private car and MaaS. To emphasize the differences, we set the use cost of private cars to 0.5 €/km to intentionally devalue the use of private cars. Two anchor nodes are chosen randomly in the study area and the comparisons are shown in Figure 6. As shown, the accessible activity locations vary between the use of private cars and MaaS in both STP and SMP. Specifically, cars have 125 accessible activity locations in STP and 47 in SMP (Figure 6(a)), while MaaS has 79 accessible activity locations in STP and 140 in SMP (Figure 6(b)). The large gaps between them highlight the inconsistency of accessibility delineated by different resource constraints. In Figure 6(a), the SMP presented by blue dots highlights that car accessibility is primarily restricted by the monetary budget (including ownership cost). Conversely, in Figure 6(b), the MaaS accessibility is primarily constrained by the time budget, and thus the STP is represented by red dots to distinguish them. In intersections of the corresponding STP and SMP, there are 47 locations for cars and 79 for
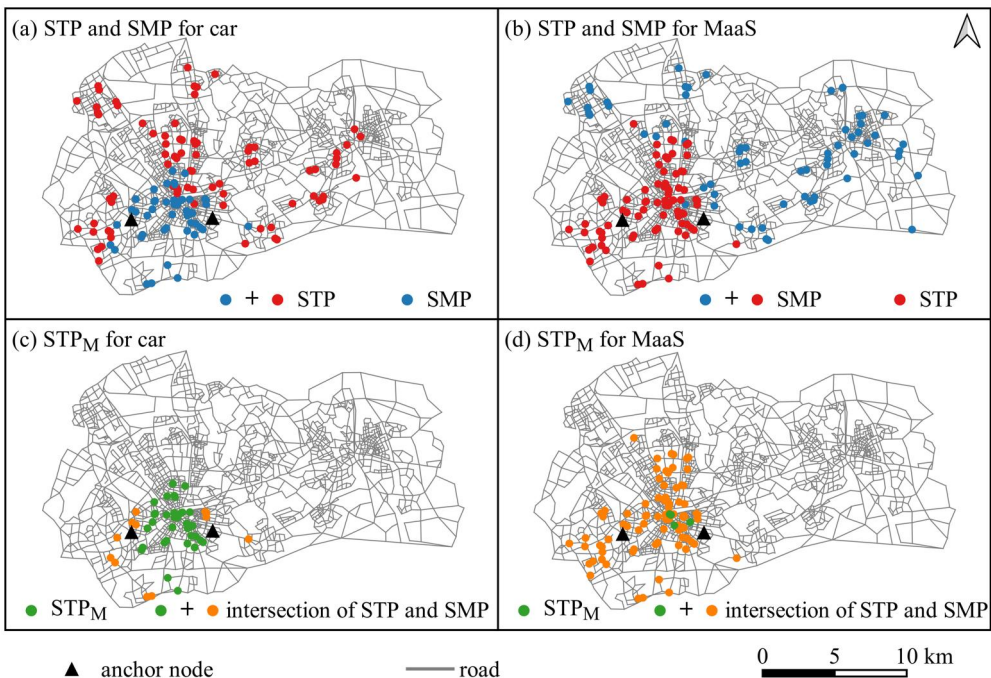

Figure 6. Comparison between STP, SMP, and STP_M for car and MaaS.

MaaS (Figure 6(c–d)). Based on the STP_M, it is surprising that 34 are accessible for cars (Figure 6(c)) but only 4 for MaaS (Figure 6(d)), which are significantly less than those delineated by the intersection method. The underlying reason is that the two resource constraints have different cost structures in the transport network, thereby invalidating the intersection method.

4.2.2. Demonstration at a population level

At a population level, we show the accessibility differences resulting from STP and STP_M. Scenario-based tests are conducted to assess the impact of different use costs. One run per scenario takes around 10 minutes on a personal computer (AMD Ryzen™ 5800H with 16 GB RAM). Finally, the Lorenz curves are shown to indicate equality in accessibility.

Individuals are classified into low-, medium-, and high-income groups following a positively skewed distribution. For each, the two anchor points are set as the home location. The allocation of a monetary budget and MaaS bundle to an individual follows the principle that a higher income level has a higher chance of a higher monetary budget and bundle level. The actual monetary budget for travel is derived by subtracting the allocated membership fees for each day from the individual monetary budget, which is as €3.0, €6.0, and €12.0 for the low-, medium-, and high-income groups, respectively. According to Andor et al. (2020), the fees for using small, medium, and large private cars are estimated as €0.15, €0.25, and €0.40 per km, respectively, corresponding to the private car use costs of three income groups. To incorporate some variations, a small subset of individuals in an income group is assigned different levels of MaaS bundles and monetary budgets. On average, the majority of individuals from an income level have a MaaS bundle and monetary budget at the same level.

We measure NAL and AFC_c, $c=\{T, M\}$, for the sample. As the measurements show similar patterns, we select NAL in the Eindhoven and Helmond cities for demonstration in Figure 7. The results reveal several insights. First, accessibility under a single constraint (i.e. time) is consistently higher than that under dual constraints (i.e. time and money) using the same transport mode, confirming the results in Section 4.2.1. that ignoring monetary budget overestimates accessibility. Second, the changes in the accessibility of bike + PT (Subfigure a–b) are relatively smaller compared to those taking car or bike + PT (if the individual does not have a car) in Subfigure c–d and MaaS in Subfigure e–f. This outcome can be attributed to the cheaper fares by PT that only exert a minor influence on monetary budget. Third, while the accessibility of MaaS and cars experience a large reduction, car accessibility is still higher than MaaS accessibility in most postcode areas. This result implies that private cars still excel in overcoming spatial separation even when MaaS has a large coverage.

Figure 8 presents the accessibility (NAL and AFC_T) resulting from STP_M using different transport modes. The sequence of postcode areas in the x-axis of Figure 8(a) is ranked in increasing order in terms of NAL, and the sequence remains the same in all other (sub)figures. The curves show that individuals traveling with a car or bike + PT (indicated by the blue curves) have the highest accessibility except for a few postcode areas, where MaaS outperforms slightly. These postcode areas are located near the
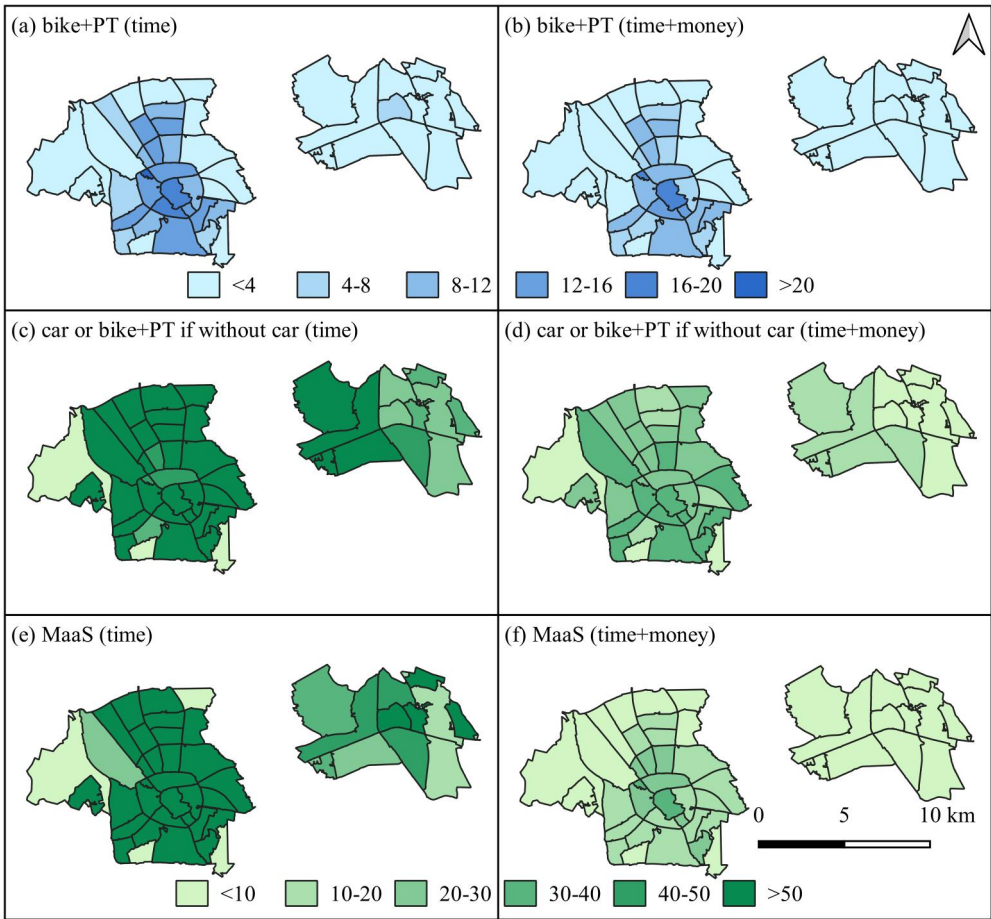
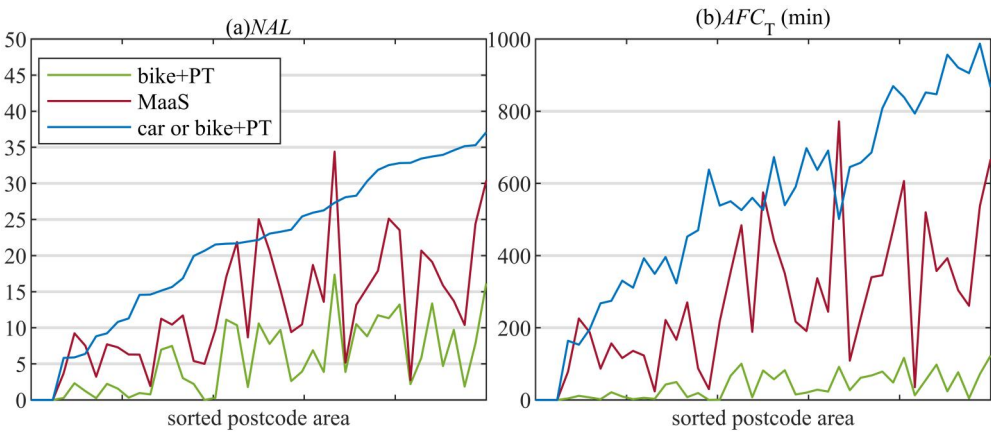**Figure 7.** *NAL* in STP and STP$_M$.

Figure 8. Accessibility based on different transport modes.

centers of Eindhoven and Helmond, where the use of cars does not have absolute travel time savings over the use of MaaS. Individuals traveling only with bike + PT receive the lowest accessibility as indicated by the green curves, implying that public transport is insufficient for competing with other modes even if facilitated by trip chaining with a bike (i.e. bike and ride). Although bike + PT involves the lowest monetary costs, the time budget constraint stands out to curtail accessibility. Note also that not everyone owns a car in the study area, implying that owning a car represents dominantly high accessibility in the study area.

Given that MaaS already has large spatial coverage, we test to what extent the costs of using private cars and MaaS influence accessibility (NAL and AFC_M) resulting from STP_M. Figure 9 illustrates the accessibility concerning different use costs. We compare the results under three scenarios: (1) MaaS is with the original bundle costs defined in Section 4.1; (2) the use costs of MaaS (excluding the membership fee) are reduced by 50%; and (3) the use costs of private cars are doubled. The results show that private car is not as competitive as the original MaaS bundles in most postcode areas, corroborating the argument that the ignorance of monetary budget constraints overestimate accessibility. On the other hand, it is found that significantly reducing the MaaS bundle costs only marginally improves accessibility with the presence of time budget constraints.

To study the effects of the monetary budget on space–time equality, Figure 10 presents the comparison of Lorenz curves under various scenarios. In both subfigures, the black dashed lines represent perfect equality while the cyan dot lines represent the Lorenz curves of NAL in STP_M considering private car (depending on ownership), bike + PT, and MaaS as mode alternatives. In Figure 10(a), the blue curve represents the NAL in STP for comparison purposes, while the red curve presents the NAL in STP_M for individuals using either car or bike + PT. In Figure 10(b), the blue and red lines present the NAL in STP_M with doubled car use costs and halved MaaS use costs, respectively, considering all available modes.

The findings can be summarized as follows. First, when considering only the time budget constraint for accessibility, with car and bike + PT as the mode alternative, the Lorenz curve deviates the least from the line of equality, with the lowest Gini
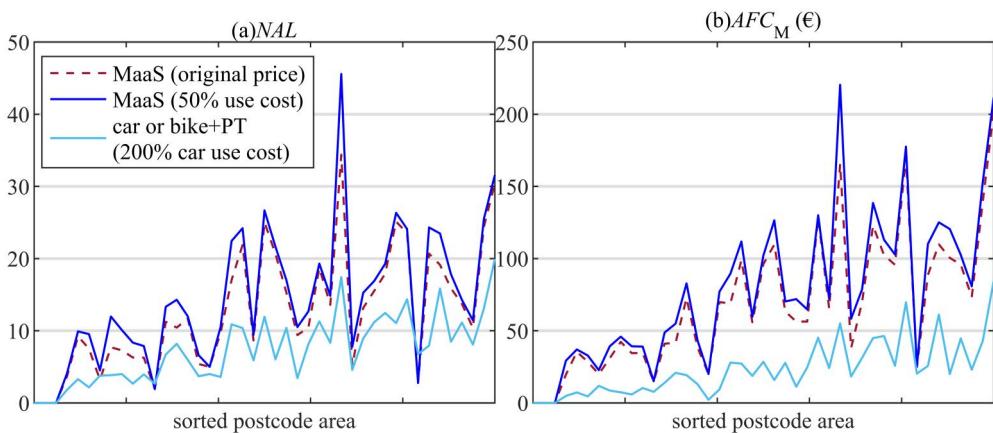

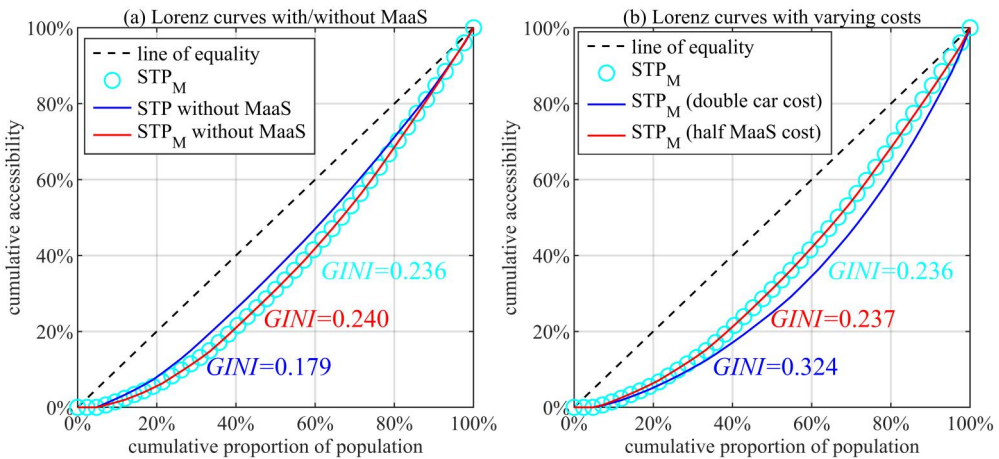**Figure 9.** Accessibility based on different costs.

Figure 10. Lorenz curves using *NAL* as the accessibility indicator.

coefficient of 0.179 (blue curve in Figure 10(a)). However, when both time and monetary budget constraints are considered, the Lorenz curves deviate further from equality, resulting in a higher Gini coefficient of 0.236 (cyan dot line in Figure 10(a)), which only has a marginal decrease in inequality compared to the situation where MaaS is not introduced (red curve in Figure 10(a)). This can be attributed to the uneven impacts of MaaS on improvement in accessibility across the population. Second, a significant increase in the use costs of private cars exacerbates inequality, as indicated by a Gini coefficient of 0.324 (blue curve in Figure 10(b)). This is possible because the introduction of higher pricing negatively affects accessibility for different segments of the population. Third, changes in the MaaS bundle, such as a 50% discount (red curve in Figure 10(b)), do not lead to improvement in equality. This can be explained by the high entry fees associated with MaaS and the existing spatial inequality, which cannot be compensated by significant pricing reductions alone for the original low-accessibility group.

According to the analysis results, it is concluded that it is necessary to consider both time and monetary budget constraints for the measurements of space−time accessibility and equality. In addition, it is found that MaaS offers improvement in accessibility in certain areas where the use of private cars is not advantageous, but it cannot effectively address the gap of inequality caused by spatial heterogeneities. Thus, the deployment of MaaS should be cautious and dedicated to those who suffer from low accessibility to mitigate accessibility disparities.

5. Conclusion and future work

This study incorporates monetary budget in STP modeling in a multimodal supernetwork. Additionally, we integrate MaaS with a complex monetary cost structure that is well-situated for assessing the impacts of monetary budget on individual potential mobility space. We develop the TBBS method for constructing individuals' STP_M efficiently. The proposed method is applied in the Eindhoven-Helmond corridor, the Netherlands to evaluate space−time accessibility and equality. The results show that

STP_M reflects more realistic potential mobility constrained by time and monetary budgets, thereby representing a high potential for analyzing accessibility and equality. The proposed STP model and solution method can be extended to incorporate other budget constraints and is feasible for large-case accessibility evaluations.

The proposed STP modeling extension paves the way for several research directions, which we will address in future work. First, the proposed STP_M only considers a single flexible activity, and it would be meaningful to expand the scope to model the potential mobility space of multimodal and multi-activity trip chains. In the presence of multiple activities, the monetary budgets are often compensative between the activities. Thus, individuals are more likely subject to the total monetary budgets for daily activity programs. Second, the deterministic modeling of time and monetary costs cannot reflect the stochastic nature of the urban and transport system. Thus, future work should take uncertain time and monetary costs into account. Third, dedicated urban policies and network strategies should be designed and analyzed to improve space–time accessibility and equality simultaneously. Fourth, the proposed space–time prism model can address the MaaS without relying on fixed stations in the free-floating scheme, by introducing the transfer links at all possible locations in the MaaS network. Nevertheless, it's noteworthy that the current study does not conduct a test of it, which can be an interesting topic for investigation in future work.

Disclosure statement

No potential conflict of interest was reported by the author(s).

Data and code availability statements

The data and codes that support the findings of this study are available on figshare.com with the identifier(s) at https://doi.org/10.6084/m9.figshare.23708532.v1.

Funding

Notes on contributors

Jing Qin is a Ph.D. candidate at the Urban Planning and Transportation Group of Eindhoven University of Technology (the Netherlands). Her research interests include space-time prism modeling, accessibility and equity measures, and transport network design. Jing Qin designed the model and the computational framework, carried out the implementation, and wrote the draft manuscript.

Feixiong Liao is an assistant professor at the Urban Planning and Transportation Group of Eindhoven University of Technology (the Netherlands). His research interests include activity-based modeling, accessibility analysis, discrete choice modeling, and supernetwork modeling for applications in urban planning and transportation research. Feixiong Liao designed the model and the computational framework, reviewed and edited the manuscript, and supervised the research.

References

Andor, M.A., et al., 2020. Running a car costs much more than people think—stalling the uptake of green travel. *Nature*, 580 (7804), 453–455.

Ben-Akiva, M., and Lerman, S.R., 1979. Disaggregate travel and mobility-choice models and measures of accessibility. *In*: D. Hensher and P. Stopher, eds. *Behavioural travel modelling*. London: Croom-Helm, 654–679.

Bittencourt, T.A., and Giannotti, M., 2021. The unequal impacts of time, cost and transfer accessibility on cities, classes and races. *Cities*, 116, 103257.

Chen, B.Y., et al., 2013. Reliable space–time prisms under travel time uncertainty. *Annals of the Association of American Geographers*, 103 (6), 1502–1521.

Conway, M.W., and Stewart, A.F., 2019. Getting Charlie off the MTA: a multiobjective optimization method to account for cost constraints in public transit accessibility metrics. *International Journal of Geographical Information Science*, 33 (9), 1759–1787.

El-Geneidy, A., et al., 2016. The cost of equity: assessing transit accessibility and social disparity using total travel cost. *Transportation Research Part A: Policy and Practice*, 91, 302–316.

Fang, Z., et al., 2011. A multi-objective approach to scheduling joint participation with variable space and time preferences and opportunities. *Journal of Transport Geography*, 19 (4), 623–634.

Ford, A., et al., 2015. Transport accessibility analysis using GIS: assessing sustainable transport in London. *ISPRS International Journal of Geo-Information*, 4 (1), 124–149.

Fu, X., et al., 2022. Measuring joint space-time accessibility in transit network under travel time uncertainty. *Transport Policy*, 116, 355–368.

Gini, C., 1909. Concentration and dependency ratios (in Italian). *Rivista di Politica Economica*, 87, 769–789.

Goldin, B., and Salzman, O., 2021. Approximate bi-criteria search by efficient representation of subsets of the pareto-optimal frontier. *Proceedings of the International Conference on Automated Planning and Scheduling*, 31, 149–158.

Hägerstrand, T., 1970. What about people in regional science? *Papers of the Regional Science Association*, 24 (1), 6–21.

Handy, S.L., and Niemeier, D.A., 1997. Measuring accessibility: an exploration of issues and alternatives. *Environment and Planning A: Economy and Space*, 29 (7), 1175–1194.

Hernández Ulloa, C., et al., 2020. A simple and fast bi-objective search algorithm. *Proceedings of the International Conference on Automated Planning and Scheduling*, 30, 143–151.

Herszenhut, D., et al., 2022. The impact of transit monetary costs on transport inequality. *Journal of Transport Geography*, 99, 103309.

Hietanen, S., 2014. Mobility as a service—the new transport model? *EuroTransport*, 12 (2), 2–4.

Horner, M.W., and Wood, B.S., 2014. Capturing individuals' food environments using flexible space-time accessibility measures. *Applied Geography*, 51, 99–107.

Kang, J.E., and Chen, A., 2016. Constructing the feasible space–time region of the household activity pattern problem. *Transportmetrica A: Transport Science*, 12 (7), 591–611.

Kuijpers, B., et al., 2010. Anchor uncertainty and space-time prisms on road networks. *International Journal of Geographical Information Science*, 24 (8), 1223–1248.

Lee, J., and Miller, H.J., 2020. Robust accessibility: measuring accessibility based on travelers' heterogeneous strategies for managing travel time uncertainty. *Journal of Transport Geography*, 86, 102747.

Liao, F., 2019. Space–time prism bounds of activity programs: a goal-directed search in multi-state supernetworks. *International Journal of Geographical Information Science*, 33 (5), 900–921.

Liao, F., 2021. Exact space–time prism of an activity program: bidirectional searches in multi-state supernetwork. *International Journal of Geographical Information Science*, 35 (10), 1975–2001.

Liao, F., Arentze, T., and Timmermans, H., 2010. Supernetwork approach for multimodal and multiactivity travel planning. *Transportation Research Record: Journal of the Transportation Research Board*, 2175 (1), 38–46.

Liao, F., Arentze, T., and Timmermans, H., 2013. Incorporating space–time constraints and activity-travel time profiles in a multi-state supernetwork approach to individual activity-travel scheduling. *Transportation Research Part B: Methodological*, 55, 41–58.

Mahmoudi, M., et al., 2019. Accessibility with time and resource constraints: computing hyperprisms for sustainable transportation planning. *Computers, Environment and Urban Systems*, 73, 171–183.

Miller, H.J., 1991. Modelling accessibility using space-time prism concepts within geographical information systems. *International Journal of Geographical Information Systems*, 5 (3), 287–301.

Neutens, T., et al., 2010. Equity of urban service delivery: a comparison of different accessibility measures. *Environment and Planning A: Economy and Space*, 42 (7), 1613–1635.

Neutens, T., et al., 2007. Human interaction spaces under uncertainty. *Transportation Research Record: Journal of the Transportation Research Board*, 2021 (1), 28–35.

O'Sullivan, D., Morrison, A., and Shearer, J., 2000. Using desktop GIS for the investigation of accessibility by public transport: an isochrone approach. *International Journal of Geographical Information Science*, 14 (1), 85–104.

Qin, J., and Liao, F., 2021. Space–time prism in multimodal supernetwork – part 1: methodology. *Communications in Transportation Research*, 1, 100016.

Qin, J., and Liao, F., 2022. Space–time prisms in multimodal supernetwork – part 2: application for analyses of accessibility and equality. *Communications in Transportation Research*, 2, 100063.

Song, Y., et al., 2017. Green accessibility: estimating the environmental costs of network-time prisms for sustainable transportation planning. *Journal of Transport Geography*, 64, 109–119.

Widener, M.J., et al., 2015. Spatiotemporal accessibility to supermarkets using public transit: an interaction potential approach in Cincinnati, Ohio. *Journal of Transport Geography*, 42, 72–83.

Winter, S., and Yin, Z.-C., 2010. Directed movements in probabilistic time geography. *International Journal of Geographical Information Science*, 24 (9), 1349–1365.

Yin, Z., et al., 2020. A spatial data model for urban spatial–temporal accessibility analysis. *Journal of Geographical Systems*, 22 (4), 447–468.

Zhang, T., et al., 2018. Quantifying multi-modal public transit accessibility for large metropolitan areas: a time-dependent reliability modeling approach. *International Journal of Geographical Information Science*, 32 (8), 1649–1676.

Appendix

Table A1. Primary notations.

Notations	Definitions
G	Transport network, $G = (V, E)$, with node set V and link set E
n	Node in G
a, A	Activity location and activity location set, $a \in A$, $A \subseteq V$
$\chi(a)$	A binary indicator showing if a is within PPA
c	Cost type, $c \in \{T, M, L\}$ in terms of time, money, and length, respectively
d_c	Minimum cost for the activity in terms of cost type c, $c \in \{T, M\}$
$[o_{cn}, u_{cn}]$	Budget window for node n in terms of cost type c, $c \in \{T, M\}$
b_c	Travel budget for cost type c, $c \in \{T, M\}$
h_0, h_1	Start and end anchor nodes
w_{c0}, w_{c1}	Value of costs at anchors in terms of cost type c, $c \in \{T, M\}$, $b_c = w_{c1} - w_{c0}$
SNK_M	Supernetwork representation for conducting the flexible activity
l_{sp}^m	Activity state s, vehicle state p, and transport mode m attached to a node in SNK_M
n^+, n^-	Successor and predecessor of node n, respectively
$N^+(n), N^-(n)$	Set of successors and predecessors of node n, $n^+ \in N^+(n)$, $n^- \in N^-(n)$, respectively
$e(\cdot, \cdot)$	A link between two neighboring nodes
ϖ_{ec}^m	Link cost of e in terms of cost type c and transport mode m
E_ρ^m	Set of transfer links to transport mode m in path ρ
β_{ec}^m	A binary indicator showing if link e is beyond the free use of m in cost type c
δ_c^m	Coefficient for converting link cost of type c into monetary cost for transport mode m
γ_e^m	A binary indicator showing if link e is an in-vehicle link for transport mode m
$\tau_c(\cdot, \cdot)$	Minimum cost between two nodes in cost type c
$\xi_c(\cdot, \cdot)$	Estimated minimum cost between two nodes in cost type c
$\rho(\cdot, \cdot)$	A path between two nodes in SNK_M, consisting of sequenced links
$\ell_{\rho c}(\cdot, \cdot)$	Cost between two nodes along path ρ in terms of cost type c
$\rightarrow, \leftarrow$	Forward and backward search directions placed on the top of a notation, respectively
$f_{\rho c}(n)$	f-Value for a path ρ between the anchor nodes through intermediate node n
F_c^m	Fixed cost of using transport mode m in terms of cost type c
$\alpha_{\rho e}^m$	A binary indicator showing if F_c^m in path ρ is included in the link cost of e
θ_c^m	Predefined amount of free use of transport mode m in cost type c
$q_k(n)$	The k-th label of node n
$z_k(n)$	Number of transfers in the k-th label of node n
Γ_f, Γ_b	Forward and backward containers to store non-dominant labels
ψ_f, ψ_b	Forward and backward containers to store selected labels from Γ_f and Γ_b
$\vartheta_c(n)$	The latest identified non-dominated label of node n

c: represents time and monetary costs, unless otherwise specified.
$(\cdot, \cdot)$: can be unattached from a notation with unspecified nodes.